Ultrafast photophysical studies of sulfonated polyaniline in aqueous medium by femtosecond transient absorption spectroscopy

Rijia Khatun, Koushik Majhi, Subrata Sinha*

Integrated Science Education and Research Centre, Siksha Bhavana, Visva-Bharati, Santiniketan – 731 235, India

*Corresponding author.

E-mail address: subratasinha67@rediffmail.com (S. Sinha).

ABSTRACT

In our previous work (Khatun et al., J. Phys. Chem. A 122 (2018) 7089-7098), synthesis and characterization of sulfonated polyaniline (SPANI) were discussed. Photophysical properties of SPANI in aqueous medium were also investigated using steady state spectroscopic techniques, which suggested the co-existence of two conformations ('A' and 'B') of SPANI in the normal working low acidic medium. Also, combined red-edge effect was observed from the two conformations of SPANI in aqueous medium. In the present work, a detailed investigation is carried out on the ultrafast photophysical properties of SPANI in aqueous medium by employing femtosecond transient absorption spectroscopy based on pump-probe technique. It is found that excited state absorption from the S_1 state of SPANI in aqueous medium to higher electronic states originates mostly due to the conformation 'A' in the whole spectral range and very weakly due to the conformation 'B' on the blue side of the spectra. These new findings are extremely important keeping in mind various potential applications of SPANI in the field of polymer optoelectronics.

Keywords:

sulfonated polyaniline

fs transient spectroscopy

ultrafast photophysical properties

excited state absorption

solvent-solute relaxation

1. Introduction

Polyaniline (PANI) is one of the most widely studied conducting polymers due to its many interesting properties like chemical and environmental stability, redox reversibility, and ease of synthesis [1]. The conducting or semiconducting nature of PANI has been used in various applications, like biosensors [2,3], supercapacitors [4], metal-semiconductor devices [5], actuators [6], secondary batteries [7,8], light emitting diodes [9], photovoltaic devices [10], field effect transistors [11], laser printing [12], anticorrosion coating [13–15], etc. However, the main drawback of PANI is its poor solubility in water [16]. Till date, the most common method to improve the solubility, and hence processability of PANI in water is sulfonation, in which the emeraldine salt form of PANI is treated with chlorosulfonic acid in an inert solvent [17–21]. The sulfonated PANI (SPANI) so prepared is water soluble at all pH values, though at the cost of conductivity to some extent due to the presence of strong electron withdrawing sulfonic acid ($-SO_3H$) groups [22].

In our previous work [23], SPANI was prepared by direct sulfonation of emeraldine salt form of PANI with chlorosulfonic acid in an inert solvent. The material characterizations of SPANI were carried out using Fourier transform infrared (FTIR) spectroscopy, X-ray diffraction (XRD) and field emission scanning electron microscope (FESEM). Detailed photophysical properties of SPANI in aqueous medium were investigated using steady state (absorption as well as fluorescence emission) and time-resolved (time-correlated single photon counting, TCSPC, set up for fluorescence lifetime measurement) spectroscopic techniques. The steady state absorption spectra of SPANI consist of a relatively sharp peak at 320 nm (3.88 eV), a shoulder at about 440 nm (2.82 eV) and a broad band at 650 nm (1.91 eV). These bands are attributed to π-π^* transition due to the benzenoid unit, polaron transition and charge transfer exciton like transition due to the

quinoid unit, respectively. The steady state fluorescence emission of SPANI in aqueous medium is due to the benzenoid unit upon photoexcitation by π-π* transition from ground singlet state to first excited singlet state ($S_0 \rightarrow S_1$), and ranges from 350 nm to 525 nm (approximately). Possibility of any excimer/aggregate formation of SPANI in aqueous medium at high concentrations of the polymer was excluded based on the concentration dependent measurements of the fluorescence emission spectra. Temperature dependent measurements of the fluorescence emission spectra of SPANI in aqueous medium indicated the possibility of dual fluorescence from two closely lying singlet (S_1) excited conformations. Again, pH dependent measurements of steady state absorption and fluorescence emission spectra suggested the co-existence of two ground state conformations ('A' and 'B') of SPANI. The conformation 'A' arises due to six-membered ring formation by H-bonding between the H atom of the sulfonic acid group and N atom of the amine group. However, the conformation 'B' arises due to abstraction of one H atom from the solvent by the amine group. The conformation 'B' was found to be relatively less stable than the conformation 'A' in the ground state. Also, it was suggested that population of conformation 'A' is more than that of conformation 'B' in less acidic medium, while the reverse is true in more acidic medium. Obviously, in normal working low acidic (pH = 4.5) aqueous medium, contribution from conformation 'A' was found to be more than that of conformation 'B' in the fluorescence emission spectra. These findings were corroborated by the data obtained from the time-resolved measurements. Moreover, excitation wavelength dependent measurements of the fluorescence emission spectra of SPANI in aqueous medium revealed combined red-edge effect (REE) from the two conformations of SPANI.

The prime objective of the present work is to investigate the sub-ns (or ultrafast) photophysical properties of SPANI in aqueous medium by carrying out femtosecond (fs)

transient absorption measurements based on pump-probe technique. The present findings are extremely important keeping in view various commercial applications of SPANI in the field of polymer optoelectronics. It is to be mentioned that till date, to the best of our knowledge, only a few literature data are available on the ultrafast spectroscopy of PANI [24-26]. Kim et al. [24,25] reported ultrafast pump-probe spectroscopic measurements of primary and secondary doped forms of PANI in solution to investigate the relaxation dynamics of photoexcited carriers and established that the excited carriers relax nonradiatively to the ground state via an intermediate state with a twisted geometry. Using fs pump-probe transient absorption measurements, Menšik et al. [26] observed and theoretically explained the ultrafast dynamics of excited state, charge transfer state and polaron state of emeraldine base form of PANI in solution.

2. Chemicals and Methods

2.1. Chemicals

Aniline hydrocholoride (SRL India), ammonium persulphate (Merck India), chlorosulfonic acid (Spectrochem India), 1,2-dichloroethane (DCE) (Spectrochem India) and millipore water (Merck India) were used as supplied without further purification. The solvent (millipore water) was tested before use and no impurity emission was detected in the wavelength region studied.

2.2. Synthesis and Characterization of SPANI

The synthesis and characterizations (material as well as optical) of SPANI were carried out as described in our previous work [23].

2.3. Set Up for Femtosecond Transient Absorption Measurement

For the pump-probe transient absorption measurements, a mode-locked automated broadband (tuning from 690 nm to 1040 nm) Ti:Sapphire laser (Mai Tai HP, Spectra Physics), pumped by 14 W frequency doubled ND:YVO_4 (532 nm), was used as master oscillator. It produces laser pulses of < 100 fs duration (full width at half-maximum, FWHM) and ~31 nJ (energy/pulse) centred at 800 nm (80 MHz repetition rate) with average power 2.5 W. A part of this fundamental pulsed laser beam was stretched in a grating stretcher and amplified at 1 kHz using a Ti:Sapphire regenerative amplifier (Spitfire Ace, Spectra Physics) pumped by the second harmonic (527 nm, 30 W) from intercavity-doubled, diode-pumped Q-switched ND:YLF laser (Empower-30 Spectra Physics). Compression of the amplified pulses yielded > 4 mJ pulses centered at 800 nm having an FWHM of < 120 fs. Part of this amplified fundamental beam was seed into OPA (TOPAS Prime) to create pump source of required wavelength for pump-probe experiment and another part of this fundamental beam (100 mW) was steered to generate a white-light continuum for generating probe pulse for transient absorption experiment. To perform pump-probe experiment, transient spectrometer of CDP Corporation (Excipro) was used. The output of TOPAS prime was used as pump source at required wavelength and fed into the spectrometer through synchronized chopper at 1 kHz repetition rate. A lens (f = 200 mm) was used to adjust the pump diameter, while an iris and neutral density filter combination were used to adjust the pump energy. A Berek's variable wave plate was placed in the pump beam for

polarization and continuum chirp measurement. A part of the (1 kHz repetition rate) amplified fundamental beam (100 mW, 800 nm) was fed to the spectrometer focused onto a thin rotating (2 mm) CaF_2 crystal window to generate a white-light continuum and a fraction of this beam was sent to a photodetector, which controls speed and phase of the chopper rotation. The beam of white light was collimated with a parabolic mirror (f = 50 mm, 90 deg). Suitable aperture cut the central part of the white light continuum and a suitable filter eliminated the fundamental light. Then this white light was reflected from a beam splitter and mirror into two identical probe and reference beams. Two concave mirrors (f = 150 nm) were used to focus both probe and reference beams to the rotating sample cell. Two lenses (f = 60 mm) made probe and reference images at the entrance surfaces of two optical fibers, which are connected to the entrance slit of the imaging spectrometer (CDP2022i). This spectrometer consists of UV-visible photodiode (Si linear photodiode) arrays and IR photodiode (GaAs linear photodiode) array with spectral response range 200-1000 nm and 900-1700 nm, respectively.

3. Results and Discussion

3.1. Transient Absorption up to a Delay Time of 1 ns

Figure 1 shows the transient absorption spectra of SPANI in aqueous medium (concentration: 0.3 mg ml^{-1}) at different delay times (up to 1 ns) following excitation (pump) at 320 nm (π-π^* transition due to the benzenoid unit, $S_0 \rightarrow S_1$). Clearly, upon excitation, fast (apparently within a few hundred fs) excited state absorption (ESA) from the S_1 state of SPANI to higher electronic states (S_n, n = 2,3,4,….) gives rise to broad transient absorption spectra in the

spectral region 425-575 nm (approximately), which then decays in the fs-ps time scale due to depopulation of the S_1 state. Apparently, the broad transient absorption spectra consist of two bands. At shorter delay times, both the bands are weak and broadly overlapping, which makes it difficult to determine the exact peak positions of the two bands. However, at longer delay times, as the band on the red side of the spectra is almost completely decayed, the peak position of the band on the blue side of the spectra becomes clear (about 474 nm). On the other hand, looking at the spectra at 650 fs delay time, the peak position of the band on the red side of the spectra may be assigned to be at about 530 nm (as the contribution from the other band is relatively weak on the red side of the spectra at this delay time).

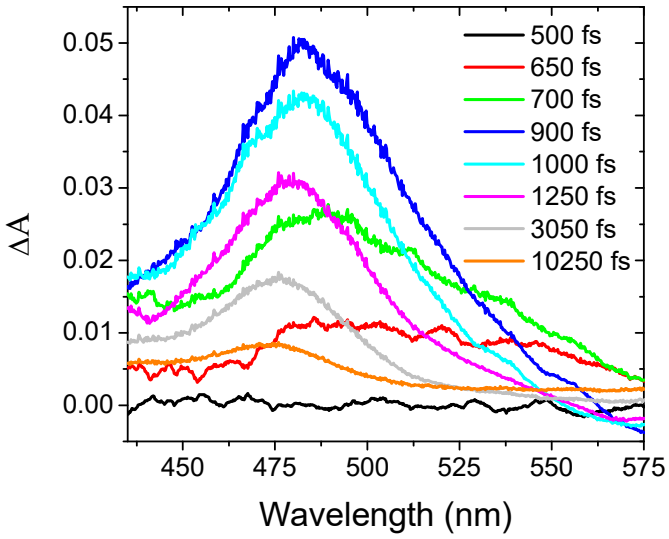

Fig. 1. Transient absorption spectra of SPANI in aqueous medium (0.3 mg ml^{-1}) at different delay times (up to 1 ns) following excitation at 320 nm with a laser pulse.

To understand the origin of these two bands in the transient absorption spectra (Fig. 1), the transient absorption kinetics are analyzed at probe wavelengths of 474 nm and 530 nm. At 474 nm, the transient absorption kinetics at shorter delay times are fitted by a single-exponential rise with a time constant of 246 fs, while the decay of the transient absorption follows a triple-exponential fit with decay time constants of 337 fs, 4106 fs and a third long-lived component having normalized pre-exponential factors 0.921, 0.063 and 0.016, respectively (Fig. 2). The third long-lived component, having a very low contribution to the overall decay curve, is neglected. Again, at 530 nm, the transient absorption kinetics follow a single-exponential rise with a time constant of 375 fs at shorter delay times (Fig. 3). The decay of the transient absorption at 530 nm follows a triple-exponential fit with decay time constants of 176 fs, 537 fs and a third long-lived component having normalized pre-exponential factors 0.994, 0.005 and 0.001, respectively (Fig. 3). The second and third decay components, having very low contributions to the overall decay curve, are neglected.

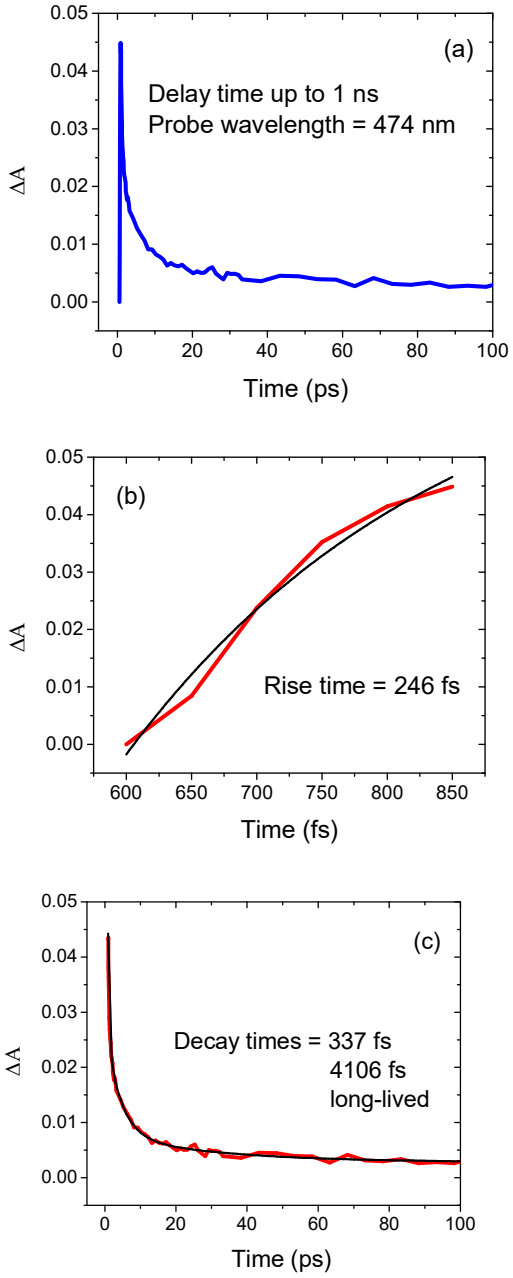

Fig. 2. Transient absorption kinetics of SPANI in aqueous medium (0.3 mg ml^{-1}) following excitation at 320 nm at a probe wavelength of 474 nm (up to a delay time of 1 ns): (a) complete transient absorption kinetics; (b) rise of the transient absorption (red curve) and single-exponential fit (black curve) (r^2 = 0.973); (c) decay of the transient absorption (red curve) and triple-exponential fit (black curve) (r^2 = 0.997).

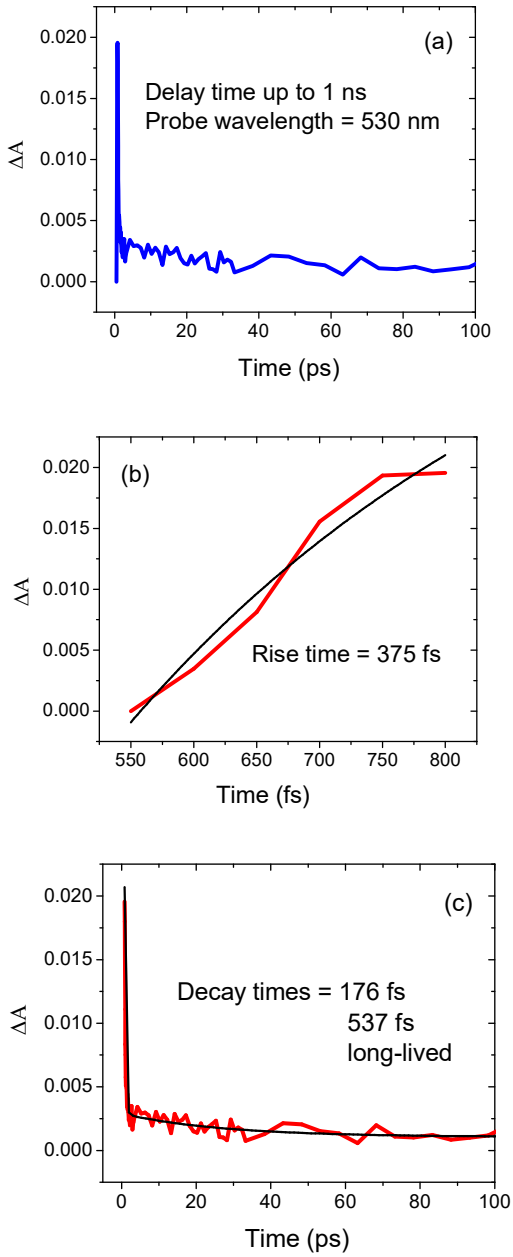

Fig. 3. Transient absorption kinetics of SPANI in aqueous medium (0.3 mg ml^{-1}) following excitation at 320 nm at a probe wavelength of 530 nm (up to a delay time of 1 ns): (a) complete transient absorption kinetics; (b) rise of the transient absorption (red curve) and single-exponential fit (black curve) (r^2 = 0.943); (c) decay of the transient absorption (red curve) and triple-exponential fit (black curve) (r^2 = 0.968).

3.2. Transient Absorption up to a Delay Time of 120 ps

Figures 2 and 3 clearly indicate that the two bands in the transient absorption spectra of SPANI in aqueous medium (Fig. 1, using different delay times up to 1 ns) follow ultrafast (of the order of few hundred fs or few ps) formation and decay kinetics. Therefore, to have a better look into the origin of these two bands, transient absorption measurements of SPANI in aqueous medium (concentration: 0.3 mg ml^{-1}) are carried out using different delay times up to 120 ps following excitation at 320 nm. The transient absorption spectra obtained from these measurements are shown in figure 4. Figure 4 shows similar features as figure 1 except that the two bands on the blue and red sides of the spectra are apparently resolved better in the former one. Accordingly, the peak positions of the bands on the blue and red sides of the spectra are assigned to be at about 471 nm and 530 nm, respectively (based on Fig. 4).

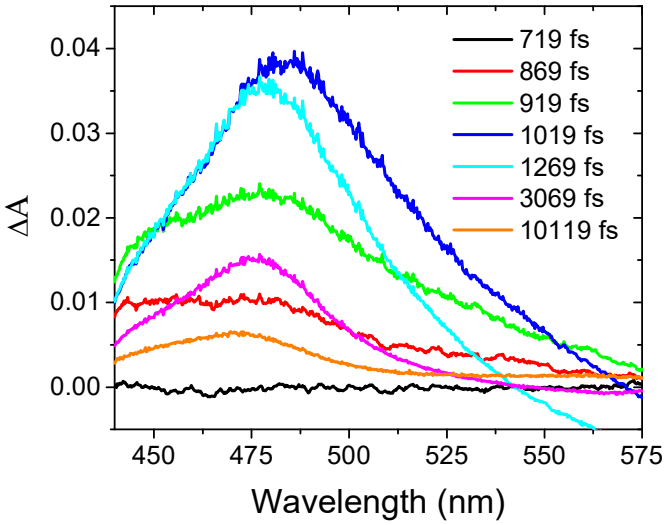

Fig. 4. Transient absorption spectra of SPANI in aqueous medium (0.3 mg ml^{-1}) at different delay times (up to 120 ps) following excitation at 320 nm with a laser pulse.

An analysis of the kinetics of the transient absorption at a probe wavelength of 471 nm in figure 4 reveals a single-exponential rise with a time constant of 138 fs at shorter delay times followed by a triple-exponential decay with decay time constants of 292 fs, 2653 fs and a third long-lived component having normalized pre-exponential factors 0.964, 0.029 and 0.007, respectively (Fig. 5). As before, the third long-lived component having a very low contribution to the overall decay curve is neglected. On the other hand, at 530 nm, the kinetics of the transient absorption follow a single-exponential rise with a time constant of 165 fs at shorter delay times, while the decay of the transient absorption perfectly follows a single-exponential decay with a time constant of 193 fs (Fig. 6).

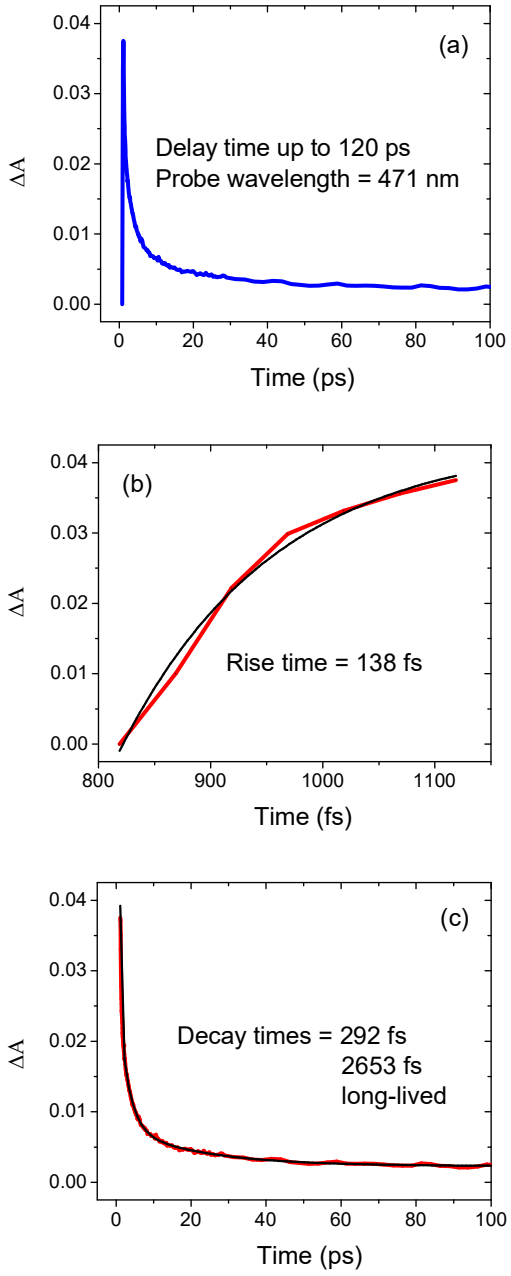

Fig. 5. Transient absorption kinetics of SPANI in aqueous medium (0.3 mg ml^{-1}) following excitation at 320 nm at a probe wavelength of 471 nm (up to a delay time of 120 ps): (a) complete transient absorption kinetics; (b) rise of the transient absorption (red curve) and single-exponential fit (black curve) (r^2 = 0.987); (c) decay of the transient absorption (red curve) and triple-exponential fit (black curve) (r^2 = 0.998).

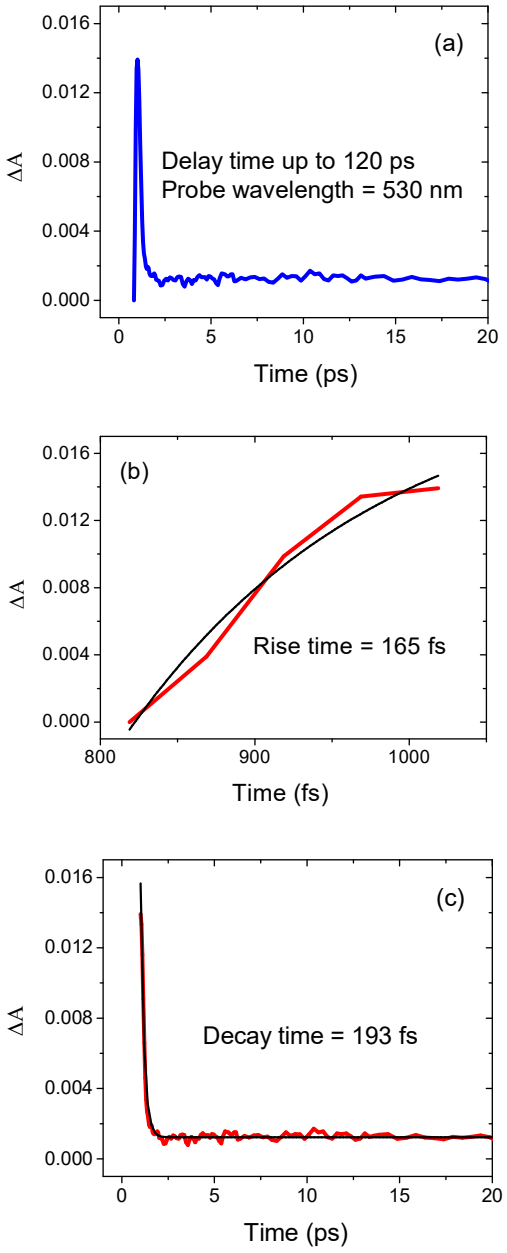

Fig. 6. Transient absorption kinetics of SPANI in aqueous medium (0.3 mg ml^{-1}) following excitation at 320 nm at a probe wavelength of 530 nm (up to a delay time of 120 ps): (a) complete transient absorption kinetics; (b) rise of the transient absorption (red curve) and single exponential fit (black curve) (r^2 = 0.949); (c) decay of the transient absorption (red curve) and triple-exponential fit (black curve) (r^2 = 0.969).

3.3. Comparative Study

From the aforementioned discussion on the transient absorption of SPANI in aqueous medium with two sets of data, one with delay time up to 1 ns as shown in figure 1 and other with delay time up to 120 ps as shown in figure 4, the following may be concluded:

(i) Upon excitation (pump) at 320 nm ($S_0 \rightarrow S_1$ transition), ultrafast ESA from the S_1 state of SPANI to higher electronic states (S_n, n = 2, 3, 4,….) gives rise to broad transient absorption spectra in the spectral region 425-575 nm (approximately), which then decays in an ultrafast time scale due to depopulation of the S_1 state. From the analysis of the kinetics of the transient absorption, it is clear that the broad transient absorption spectra of SPANI in aqueous medium consist of two bands.

(ii) The band on the blue side of the transient absorption spectra rises in an ultrafast time scale (of the order of a few hundred fs) and then decays following mainly two ultrafast time scales, first being of the order of a few hundred fs and the second is of the order of a few ps. However, the contribution of the second long-lived decay component to the overall decay profile is much smaller, though not negligible, compared to that of the first short-lived decay component.

(iii) The band on the red side of the transient absorption spectra rises in an ultrafast time scale, of the order of a few hundred fs, and then decays following mainly one ultrafast time scale, of the order of a few hundred fs. The latter is clear from the analysis of the decay profile of the transient absorption at a probe wavelength of 530 nm from the set of data using different delay times up to 120 ps.

(iv) Analysis of the two sets of transient absorption data (one with delay time up to 1 ns as shown in figure 1 and other with delay time up to 120 ps as shown in figure 4), reveals nearly similar observations. However, a careful look at the transient absorption kinetics and

corresponding fits (rise at shorter delay times and subsequent decay) clearly indicates that the rise and decay time constants are quantitatively more precise from the set of data with delay time up to 120 ps than those from the other set of data with delay time up to 1 ns.

3.4. Origin of ESA

Finally, present observations regarding the ultrafast transient absorption kinetics of SPANI in aqueous medium, keeping in mind greater precision of the data obtained from the set with delay time up to 120 ps, allow us to conclude the following: Upon photoexcitation (pump) at 320 nm ($S_0 \rightarrow S_1$ transition), ESA occurs from the S_1 state of SPANI to higher electronic states (S_n, n = 2, 3, 4,….) giving rise to a broad transient absorption spectra within the approximate range of 425-575 nm, with a rise time of 138 fs and 165 fs on the blue side (probe wavelength = 471 nm) and red side (probe wavelength = 530 nm) of the spectra, respectively. Clearly, the rise time constant remains nearly the same for the whole spectral region.

However, the decay of the transient absorption follows different kinetics on the blue side and the red side of the spectra. On the blue side, mainly two decay times are observed: one is very short-lived (292 fs) and the other is short-lived (2653 fs) with normalized pre-exponential factors 0.964 and 0.029, respectively. The very short-lived decay component (decay time ~ 292 fs) is attributed to solvent-solute relaxation (SSR), from an unrelaxed Franck-Condon excited state S_1 just after photoexcitation to a relaxed Franck-Condon excited state (relaxed S_1). Both the conformations ‘A’ and ‘B’ of SPANI undergo nearly the same extent of SSRs. The short-lived decay component (decay time ~ 2653 fs) is attributed to further stabilization of the excited state (relaxed S_1 via SSR) in energy to final excited state (final relaxed S_1) due to the enhanced conjugation for the conformation ‘B’. However, the contribution of the short-lived decay

component to the overall decay profile is much less compared to that of the very short-lived decay component. This fact agrees with our earlier observations that in normal working low acidic (pH = 4.5) aqueous medium, population of the conformation 'A' is more than that of the conformation 'B' [23]. Again, on the red side, only one very short-lived decay time (193 fs) is observed, which is ascribed to be due to the usual SSR of the conformation 'A'. Clearly, the value of the very short-lived decay time is nearly the same (~ 200-300 fs) on the whole spectral region of the transient absorption.

These observations seemingly indicate that ESA from the S_1 state of SPANI in aqueous medium to higher electronic states originates from the following:

(i) Mostly due to the conformation 'A' in the whole spectral region with rise time (τ_r) ~ 138-165 fs and decay time (τ_{d1}) ~ 193-292 fs due to usual SSR.

(ii) Very weakly due to the conformation 'B' on the blue side of the spectra with rise time (τ_r) ~ 138 fs and decay times (τ_{d1}) ~ 292 fs due to usual SSR, (τ_{d2}) ~ 2653 fs due to further stabilization for enhanced conjugation.

These various ultrafast rise and decay channels for the transient absorption of SPANI in normal working low acidic aqueous medium due to conformations 'A' and 'B' are shown schematically in figure 7.

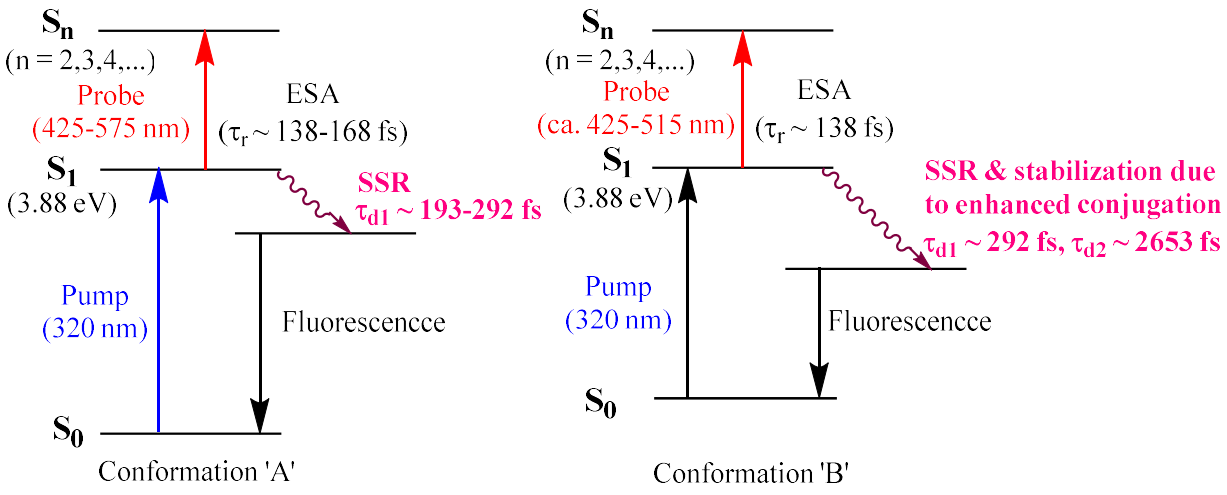

Fig. 7. Schematic diagram showing various ultrafast rise and decay channels for the transient absorption of SPANI in normal working low acidic (pH = 4.5) aqueous medium due to conformations 'A' and 'B'.

4. Conclusions

It has been already suggested [23] that two conformations ('A' and 'B') of SPANI co-exist in the ground state and first excited singlet state (S_1) in aqueous medium. The conformation 'A' arises due to six-membered ring formation by H-bonding between the H atom of the sulfonic acid group and N atom of the amine group. However, the conformation 'B' arises due to abstraction of one H atom from the solvent by the amine group. In the present work, ultrafast photophysical properties of SPANI in aqueous medium are studied in detail using fs transient absorption spectroscopy based on pump-probe technique. Two sets of measurements are carried out at different delay times, one up to a delay time of 1 ns and another up to a delay time of 120 ps, following excitation (pump) at 320 nm (S_1 state). Both the measurements give nearly similar observations regarding the formation and decay of the ESA (responsible for the transient

absorption) from the S_1 state of SPANI to higher electronic states in normal working low acidic (pH = 4.5) aqueous medium. However, quantitatively more precise data is obtained from the measurements for different delay times up to a delay time of 120 ps. Thus, it may be concluded that the aforementioned ESA originates mostly due to the conformation 'A' in the whole spectral region (with rise time ~ 138-165 fs and decay time ~ 193-292 fs) and very weakly due to the conformation 'B' on the blue side of the spectra (with rise time ~ 138 fs and decay times ~ 292 fs, 2653 fs). The very short-lived decay component (~ 193-292 fs) is attributed to SSR from unrelaxed Franck-Condon excited state to relaxed Franck-Condon excited state for both the conformations 'A' and 'B', while the short-lived decay component (~ 2653 fs) is attributed to further stabilization of the excited state (relaxed S_1 via SSR) in energy to final excited state (final relaxed S_1) due to enhanced conjugation for the conformation 'B'.

Declaration of Competing Interest

The authors declare that they have no known competing financial interests or personal relationships that could have appeared to influence the work reported in this paper.

Acknowledgements

Subrata Sinha acknowledges the Council of Scientific and Industrial Research (CSIR), India (Project No.: 03(1365)/16/EMR-II) for providing financial assistance in the form of grant. Also, SS thanks Dr. Prakriti Ranjan Bangal (Inorganic and Physical Chemistry Division, Indian

Institute of Chemical Technology, Hyderabad – 500 607, India) for the transient absorption measurements.

References

[1] V.J. Babu, S. Vempati, S. Ramakrishna, Conducting polyaniline-electrical charge transportation, Mater. Sci. Appl. 04 (2013) 1–10, https://doi.org/10.4236/msa.2013.41001.

[2] R.K. Agrawalla, V. Meriga, R. Paul, A.K. Chakraborty, A.K. Mitra, Solvothermal synthesis of a polyaniline nanocomposite – a prospective biosensor electrode material, Express Polym. Lett. 10 (2016) 780–787.

[3] Z.M. Tahir, E.C. Alocilja, D.L. Grooms, Polyaniline synthesis and its biosensor application, Biosens. Bioelectron. 20 (2005) 1690–1695. https://doi.org/10.1016/j.bios.2004.08.008.

[4] V. Gupta, N. Miura, Polyaniline/single-wall carbon nanotube (PANI/SWCNT) composites for high performance supercapacitors, Electrochim. Acta. 52 (2006) 1721–1726, https://doi.org/10.1016/j.electacta.2006.01.074.

[5] P.C. Ramamurthy, A.M. Malshe, W.R. Harrell, R.V. Gregory, K. McGuire, A.M. Rao, Polyaniline/single-walled carbon nanotube composite electronic devices, Solid State Electron. 48 (2004) 2019–2024, https://doi.org/10.1016/j.sse.2004.05.051.

[6] M. Tahhan, V.-T. Truong, G.M. Spinks, G.G. Wallace, Carbon nanotube and polyaniline composite actuators, Smart Mater. Struct. 12 (2003) 626–632, https://doi.org/10.1088/0964-1726/12/4/313.

[7] S. Venkatachalam, P.V. Prabhakaran, Oligomeric phthalocyanine modified polyaniline - an electrode material for use in aqueous secondary batteries, Synth. Met. 97 (1998) 141–146, https://doi.org/10.1016/S0379-6779(98)00125-8.

[8] K.S. Ryu, K.M. Kim, S.-G. Kang, G.J. Lee, J. Joo, S.H. Chang, Electrochemical and physical characterization of lithium ionic salt doped polyaniline as a polymer electrode of lithium secondary battery, Synth. Met. 110 (2000) 213–217, https://doi.org/10.1016/S0379-6779(99)00288-X.

[9] G. Gustafsson, Y. Cao, G.M. Treacy, F. Klavetter, N. Colaneri, A.J. Heeger, Flexible light-emitting diodes made from soluble conducting polymers, Nature. 357 (1992) 477–479, https://doi.org/10.1038/357477a0.

[10] R. Valaski, F. Muchenski, R.M.Q. Mello, L. Micaroni, L.S. Roman, I.A. Hümmelgen, Sulfonated polyaniline/poly(3-methylthiophene)-based photovoltaic devices., J. Solid State Electrochem. 10 (2006) 24–27, https://doi.org/10.1007/s10008-005-0648-8.

[11] K.F. Seidel, L. Rossi, R.M.Q. Mello, I.A. Hümmelgen, Vertical organic field effect transistor using sulfonated polyaniline/aluminum bilayer as intermediate electrode, J. Mater. Sci. Mater. Electron. 24 (2013) 1052–1056, https://doi.org/10.1007/s10854-012-0876-5.

[12] M. Kandyla, C. Pandis, S. Chatzandroulis, P. Pissis, I. Zergioti, Direct laser printing of thin-film polyaniline devices, Appl. Phys. A. 110 (2013) 623–628, https://doi.org/10.1007/s00339-012-7127-8.

[13] A. Mirmohseni, A. Oladegaragoze, Anti-corrosive properties of polyaniline coating on iron, Synth. Met. 114 (2000) 105–108, https://doi.org/10.1016/S0379-6779(99)00298-2.

[14] C.-H. Chang, T.-C. Huang, C.-W. Peng, T.-C. Yeh, H.-I. Lu, W.-I. Hung, C.-J. Weng, T.-I. Yang, J.-M. Yeh, Novel anticorrosion coatings prepared from polyaniline/graphene composites, Carbon N. Y. 50 (2012) 5044–5051, https://doi.org/10.1016/j.carbon.2012.06.043.

[15] Z. Tian, H. Yu, L. Wang, M. Saleem, F. Ren, P. Ren, Y. Chen, R. Sun, Y. Sun, L. Huang, Recent progress in the preparation of polyaniline nanostructures and their applications in anticorrosive coatings, RSC Adv. 4 (2014) 28195, https://doi.org/10.1039/c4ra03146f.

[16] S.F.S. Draman, R. Daik, A. Musa, Synthesis and fluorescence spectroscopy of sulphonic acid-doped polyaniline when exposed to oxygen gas, Int. J. Chem. Mol. Nuc. Mat. Metall. Eng. 3(2009) 183-190, https://doi.org/10.5281/ZENODO.1063288.

[17] S. Ito, K. Murata, S. Teshima, R. Aizawa, Y. Asako, K. Takahashi, B.M. Hoffman, Simple synthesis of water-soluble conducting polyaniline, Synth. Met. 96 (1998) 161–163, https://doi.org/10.1016/S0379-6779(98)00074-5.

[18] J. Yue, Z.H. Wang, K.R. Cromack, A.J. Epstein, A.G. MacDiarmid, Effect of sulfonic acid group on polyaniline backbone, J. Am. Chem. Soc. 113 (1991) 2665–2671, https://doi.org/10.1021/ja00007a046.

[19] H.S. Nalwa, Handbook of Organic Conductive Molecules and Polymers, John Wiley & Sons, England, 1997.

[20] K. Takahashi, K. Nakamura, T. Yamaguchi, T. Komura, S. Ito, R. Aizawa, K. Murata, Characterization of water-soluble externally HCl-doped conducting polyaniline, Synth. Met. 128 (2002) 27–33, https://doi.org/10.1016/S0379-6779(01)00660-9.

[21] H. Zhang, H.X. Li, H.M. Cheng, Water-soluble multiwalled carbon nanotubes functionalized with sulfonated polyaniline, J. Phys. Chem. B. 110 (2006) 9095–9099, https://doi.org/10.1021/jp060193y.

[22] V. Meriga, S. Valligatla, S. Sundaresan, C. Cahill, V.R. Dhanak, A.K. Chakraborty, Optical, electrical and electrochemical properties of graphene based water soluble polyaniline composites, J. Appl. Polym. Sci. 132 (2015) 42677, https://doi.org/10.1002/app.42766.

[23] R. Khatun, K. Majhi, V. Meriga, A.K. Chakraborty, S. Sinha, Detail photophysical studies of sulfonated polyaniline in aqueous medium, J. Phys. Chem. A. 122 (2018) 7089–7098, https://doi.org/10.1021/acs.jpca.8b06640.

[24] J. Kim, A.N. Unterreiner, S. Rane, S. Park, J. Jureller, L. Book, Y.-H. Liau, N.F. Scherer, Ultrafast dephasing of photoexcited polarons in primary doped polyaniline, J. Phys. Chem. B, 106 (2002) 12866-12873.

[25] J. Kim, S. Park, N.F. Scherer, Ultrafast dynamics of polarons in conductive polyaniline: comparison of primary and secondary doped forms, J. Phys. Chem. B, 112 (2008) 15576–15587.

[26] M. Menšik, D. Rais, J. Pfleger, Time resolved excitation dynamics in emeraldine base, Chemical Physics, 456 (2015) 79–84.